Stochastic simulation of molecular-beam epitaxial growth of a model compound semiconductor: Effects of kinetics

T. Kawamura, Akiko Kobayashi, and S. Das Sarma

Department of Physics, University of Maryland, College Park, Maryland 20742-4111

(Received 20 October 1988)

A stochastic Monte Carlo simulation is employed to study various aspects of molecular-beam epitaxial (MBE) growth with the emphasis on understanding the effects of kinetic parameters. In particular, we examine the growth profile of a model III-V compound semiconductor of an anion-terminated (001) substrate. The parameter values for the simulation were chosen with GaAs in mind. We study the effects of substrate temperature and of various kinetic rates on the multilayer growth profile. In addition, we investigate the effects of growth interruption and laser-assisted evaporation of the anion species. The emphasis in this paper is on understanding qualitative trends of MBE growth, rather than on detailed quantitative understanding of the growth of a particular material.

I. INTRODUCTION

Recently there have been many significant experimental advances in the growth of III-V compound semiconductor structures, particularly by the molecular-beam epitaxy (MBE) method. Due to the great complexity of MBE growth processes, the study of such growth mechanisms is not amenable to a first-principles theoretical analysis. Therefore, it is desirable to devise some numerical method whereby one can gain some insight into the important dynamical factors involved in MBE growth.

In this paper we study the important dynamical processes responsible for the molecular-beam epitaxial growth of model III-V semiconductor compounds. We are mainly interested in the general qualitative trends one can observe in the growth profile. We employ a direct stochastic Monte Carlo approach which has been successfully used in the study of nucleation growth of thin films by vapor deposition.[1-4] More recently, a similar technique has been used by Madhukar et al. to simulate MBE growth,[5,6] and in particular to understand the temporal oscillations in the specular beam of reflection high-energy electron diffraction (RHEED) measurements.[7,8] One of the conclusions they have reached is that there is a correspondence between the RHEED oscillations and the As_2 dissociation rate. Related work along these lines has also been done by Clarke and Vvedensky,[9] In contrast to Madhukar et al. they study a simple model system and identify the RHEED oscillations with the variation in step density of a growing sample with time. In spite of the controversial issue regarding the origin of the RHEED oscillations, we do not concern ourselves with RHEED measurements in his paper. Rather, our study is focused on the qualitative growth trends in terms of kinetic rates, parameter values, and various growth methods.

Our simulation is close in spirit to the methods used by Salik[4] and Clarke and Vvedensky,[9] in that we make use of a random-number generator to simulate atomic deposi-

tion and diffusion. However, unlike Salik's work, in our simulation the frequency of a particular dynamic process occurring is controlled by the associated kinetic rate. These rates are obtained via a simple energetics calculation, which is similar to the method used by Abraham and White.[1] In addition, we deal with two different atomic species impinging on a more complicated lattice geometry than that employed in previous work.[1-4] The anion adsorption scheme we use is similar to that used by Madhukar and collaborators. [Their scheme has been referred to as configuration-dependent reactive incorporation[5-8] (CDRI).] However, our resultant growth profiles which we display in Sec. III look different from those obtained by Madhukar et al., and are more reminiscent of the results obtained from molecular-dynamics simulations.[10]

Our growth simulation should not be taken as a quantitative study of any particular semiconductor. In fact, due to the lack of information about the various kinetic parameters such as diffusion rates, it is unlikely that a quantitative theory for the nonequilibrium MBE growth of GaAs or other such semiconductor materials will be available in the near future. We will choose the basic physical parameters for our simulation with GaAs in mind. By a simple alteration of the main simulation program we are able to investigate trends in the growth profile under various external conditions (e.g., growth interruption, laser evaporation, etc.).

Let us emphasize that for our stochastic Monte Carlo simulation to describe successfully the MBE growth of a specific material (e.g., GaAs), the activation energies for various atomistic processes must be known with some degree of accuracy. One of the major difficulties is that these various activation energies are, in general, not accurately known for the semiconductor materials of interest. Unfortunately, there is very limited reliable quantitative experimental information on atomistic surface diffusion activation energies for semiconductors. In view of these problems we have been forced to employ a very simple

(and rather drastic) approach (as explained in Sec. II A) to obtain the atomistic activation energies. In view of this simple-minded choice of activation energies our work should be taken as a feasibility study of the qualitative trends in MBE growth, rather than a realistic study of a specific material. We will, therefore, present our MBE growth results using three different sets of kinetic parameters so that one has some idea about how changing various rates affects the MBE growth quality.

II. OUTLINE OF THE STOCHASTIC MONTE CARLO SIMULATION

It is conceptually rather straightforward to apply the stochastic Monte Carlo technique to the simulation of molecular-beam epitaxial growth. One first lists all the participating kinetic processes, and ascribes to each a corresponding rate of occurrence. These rates, assumed to be of the Arrhenius form, are obtained from an energetics calculation that makes use of the cohesive energy of the semiconductor in question, and Harrison's scaling law for bond strengths.[11] Once all these rates are calculated, the simulation proceeds to activate the kinetic events corresponding to these rates and follow the individual atomic movements. The coverage of each layer can be recorded as a function of time, providing us with a multilayer growth profile for later study.

In our simulation, the following major assumptions are made.

(1) The adsorption of the atoms occurs at specific lattice sites within the zinc-blende structure (i.e., discrete lattice-gas model). At first, the zinc-blende structure of a semiconductor may appear to be a cumbersome geometry to simulate. However, upon closer investigation we see that in the [001] direction each layer is simply a square sublattice which is offset from the layer above and from the layer below by $(\sqrt{2}/4)a$, where a is the length of the conventional cubic cell. One notices that the offset of a particular corner in the square sublattice is cyclic as one progresses in the direction perpendicular to the (001) planes (see Fig. 1). In our simulation this realization greatly facilitates the indexing of the atoms as they get

FIG. 1. (a) The zinc-blende structure, and (b) the cyclic offset of a particular corner as one looks along the z direction which is perpendicular to the (001) planes. Note that all the atoms in the dashed circle have the same x-y coordinates; only their layer numbers differ.

adsorbed and move about on the crystal surface.

(2) The growth occurs on a perfect As-terminated (001) GaAs substrate. Note that we will be using the terms gallium and arsenic as the representative constituents of a III-V semiconductor compound. We simply use the terms Ga and As interchangeably with the terms cation and anion, respectively, since we will be calculating the necessary dynamic rates with GaAs in mind.

(3) We assume that the temperatures employed in our simulation are within the epitaxial window. Note that, due to the discrete nature of the lattice-gas model, we cannot simulate negative growth features such as amorphous growth which occurs at low temperatures.

(4) For the temperature range we will be investigating, we assume that evaporation from the surface is negligible. This is a valid approximation in view of the actual experimental growth situation.

(5) We ignore the diffusive processes in the upward z direction. These hopping mechanisms become important only at higher temperatures and lead to a rough islanding growth mode.

(6) We assume that there are no anion-cation substitutions during the growth (i.e., no antisite defects are allowed in our simulation).

The growth profile (i.e., the coverage per layer versus time) is recorded for a lattice size of $20 \times 20 \times 11$, meaning the square sublattices are 20×20 and there are 11 layers of such planes. Periodic boundary conditions are imposed on the xy planes such that $x_{n+1} = x_1$ and $y_{n+1} = y_1$, where n is the chosen lattice size. We have systematically changed our system size (up to 80×80) in a few cases to ensure that finite-size effects are not an important source of error in our simulation.

In our simulation we keep track of all the diffusive processes which take place within the next-nearest-neighbor distances from a given site. Since we are not allowing any anion-cation substitutions, a given atom can make the following diffusive hops, as illustrated in Fig. 2.

(i) An intralayer hop to an adjacent vacant site within the square sublattice, or

(ii) an interlayer hop downward to any one of the vacant four next-nearest-neighbor sites.

For the cations, only isolated atoms in a square sublattice are able to participate in any of the allowed intralayer or interlayer hops. These isolated atoms are allowed to migrate about the lattice until they attach to an edge of any clusters that have formed on the surface. This model is physically reasonable, since the potential to capture an atom is strong at such cluster edges, and clusters are far less mobile than isolated atoms. We note that the above mechanism of "edge progression" has been elucidated in the molecular-dynamics simulation of the Lennard-Jones system by Paik et al.[12] (See Ref. 4 for a quantitative analysis and justification for the edge-progression model.)

For the anions it is necessary to allow a greater degree of freedom, since they arrive on the surface as molecules (e.g., As$_2$). Therefore, we allow an anion which is singly bonded to an adjacent anion within the same square sublattice to first dissociate and then diffuse. Atoms which are already supporting an atom in a higher layer are not
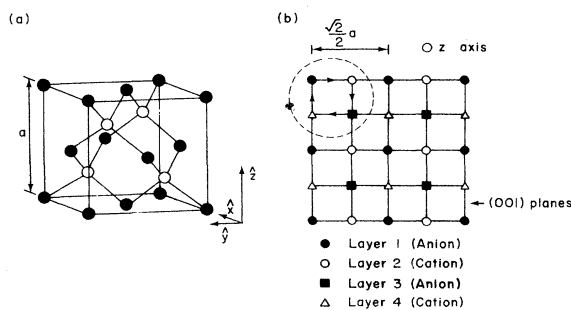
● Site at layer n

■ Site at layer n−2
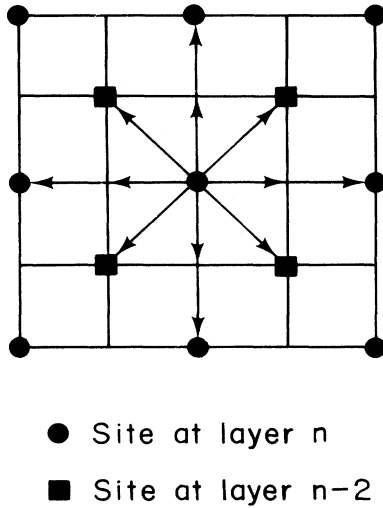
FIG. 2. The possible intralayer and interlayer diffusive hops an atom can make.

considered candidates for any diffusive process. In other words, we neglect bulk diffusion. This can be justified on the basis of the fact that bulk diffusion rates are an order of magnitude lower than surface diffusion rates. The simulation results we present here are therefore indicative only of the characteristics resulting from surface diffusion effects during growth.

A. Calculation of the rates

The kinetic rates are assumed to be of Arrhenius form:

$$R = R_0 \exp(-E/k_B T) , \tag{1}$$

where R_0 is the diffusion prefactor in hops per second. In this form, E is the activation energy barrier, that is, the energy associated with bonds that need to be broken in order for an atom to migrate into one of its neighboring sites. Thus, E is determined by the surrounding atomic configuration that is local and specific to that atom at that particular time.

In order to calculate the rates for all the diffusive processes, we first estimate the strengths of the anion-anion, anion-cation, and cation-cation bond strengths. We assume that the contributions to a typical bond strength in our model semiconductor compound are given by the interaction between the central atom and its nearest-neighbor atom plus the corresponding three next-nearest-neighbor atoms. For example, in the case of a Ga atom as the central atom, we have

$$E_c = V(\text{Ga-As}) + 3V(\text{Ga-Ga}) , \tag{2}$$

where E_c is the cohesive energy per bond, and $V(\text{Ga-Ga})$ and $V(\text{Ga-As})$ denote the cation-cation and cation-anion bond strengths, respectively.

Taking the length of the conventional cubic cell to be a, the nearest-neighbor distance in the zinc-blende structure is given by $(\sqrt{3}/4)a$, and the next-nearest-neighbor

distance is given by $(\sqrt{2}/2)a$. Making the assumption that $V(\text{Ga-Ga}) = V(\text{As-As})$, we arrive at the following relationships between the cohesive energies and bond strengths from Harrison's scaling law:

$$V(\text{Ga-Ga}) = V(\text{As-As}) = \tfrac{3}{17} E_c , \tag{3}$$

$$V(\text{Ga-As}) = \tfrac{8}{17} E_c . \tag{4}$$

Using the value $E_c = 1.63$ eV for the cohesive energy (per bond) of GaAs,[11] we have $V(\text{Ga-Ga}) = 0.77$ eV and $V(\text{Ga-Ga}) = V(\text{As-As}) = 0.29$ eV.

Once the bond strengths are calculated, we are able to calculate the activation barrier that a given atom must overcome in each of the dynamic processes. All the energy calculations take the following basic form:

$$E = F_1 [(1 \text{ or } 2)V_{\text{NN}} + F_2 V_{\text{NNN}}] , \tag{5}$$

where $V_{\text{NNN}} = V(\text{cation-cation}) = V(\text{anion-anion})$, and $V_{\text{NN}} = V(\text{cation-anion})$. The factors F_1 and F_2 are adjustable parameters. If $F_1 = 1$, then Eq. (5) represents the activation barrier for evaporation. Therefore, we must have the constraint $0 < F_1 < 1$ in order to describe diffusion. The parameter F_2 can be thought of as the average number of next-nearest neighbors an atom has during the simulation run. We use $F_1 = 0.7$ and $F_2 = 2.0$ in our simulation.

From the form of Eq. (5) we see that all the rates in our simulation are divided into two major categories: those that refer to atoms which are supported by one bond underneath, and those that are supported by two atoms. In Eq. (1) the prefactor can be chosen to be different for the anions and cations; $R_0(\text{As})$ and $R_0(\text{Ga})$. We should point out that our particular way of choosing the Arrhenius parameters preserves the microscopic reversibility (i.e., the local principle of detailed balance) even though there may not be an overall global thermodynamic equilibrium.

We point out again that this particular way of choosing our diffusion parameters and activation energies is very simple-minded and probably inadequate for quantitative details. First, the use of Harrison's scaling relation on the bond strengths is questionable, as these interactions do not "want" to occur within a tetrahedral structure. Second, the diffusion activation energy obtained from the full potential-energy surface generally differs considerably from that obtained from a simple bond-breaking argument. Finally, the dynamic activation energy for surface diffusion can be much smaller than that obtained from the static potential-energy surface. Obtaining the realistic activation energies for a system like GaAs from first-principles calculations is quite beyond the scope of the current theoretical and computational state-of-the-art techniques; it may be possible to obtain experimental information on these activation energies in the future. At present, our studies should be taken as qualitative studies of various trends only.

Once all the rates are calculated in this fashion, the incremental time unit for the simulation run must be determined. Note that the reciprocal of each rate gives us a

basic time interval unit Δt_i for each process (i) to occur once. In addition, an important time scale in the simulation is given by the cation deposition rate which is chosen to be one monolayer of growth per second. This is consistent with experimental situations. Once all the time units Δt_i are determined from the rates, the smallest one of them is chosen as the incremental time unit for the simulation. This procedure ensures proper sequencing of all the subroutines which carry out the kinetic processes involved. Thus, if the computer time is given by t, the next iteration through the subroutine loop is set to $t = t + \min(\Delta t_i)$. A flowchart of the way in which the basic incremental unit of time is determined is given in Fig. 3.

At first it may seem that any convenient time increment Δt may be chosen to advance the computer time. However, an arbitrary choice may lead to an undesirable sequencing of the kinetic processes in the simulation. Suppose that for a diffusive process (i) we have $\Delta t_i \ll \Delta t$, where Δt_i is the basic time interval for process (i) to occur once. Ideally, we would like the subroutine responsible for carrying out the kinetic process (i) to be called on when $t = n(\Delta t_i)$, with n an integer. However, since $\Delta t \gg \Delta t_i$ the process (i) will not be activated at all for times $n(\Delta t) < t < (n+1)\Delta t$. When $t = n(\Delta t)$, the program calculates the number of times a specific kinetic process should have occurred from the corresponding Arrhenius rate. This number is given by $N = (\Delta t / \Delta t_i)$, which may be quite large. Thus, process (i) is artificially "bunched up" at the arbitrarily set incremental times

$t = n(\Delta t)$, instead of being uniformly carried out at its own natural time intervals given by $t = n(\Delta t_i)$. To avoid these problems, one might set the incremental time unit to be much smaller than any of the time units associated

FIG. 4. The multilayer growth profile for the standard MBE growth method. The temperature is $T = 500$ K and the prefactor ratios $R_0(\text{Ga})/R_0(\text{As})$ are (a) 10^3, (b) 1, (c) 10^{-3}. The initial growth profile is that of the first layer of gallium growth.

Enter parameter values for initialization of simulation. Enter T, R_0(Ga), R_0(As), F1, F2, and size of the lattice

↓

Calculate all the rates for the diffusive processes.
$R_i = R_0$(Ga or As) exp(-E/kT)

↓

Calculate the basic time units for the diffusive processes
$\Delta t_i = 1 / R_i$

↓

Bubblesort all the time units,
$\Delta t_1, \Delta t_2, \Delta t_3, \cdots$ etc.
where $\Delta t_1 \leq \Delta t_2 \leq \Delta t_3 \cdots$

↓

Set the incremental time unit to $\Delta t = \Delta t_1$

↓

Enter main body of multilayer growth simulation program

→ Increment computer time
$t = t + \Delta t$
Iterate through main body of simulation program again

FIG. 3. Flowchart which shows the method by the which the simulation determines the basic incremental time unit.

with all the operative kinetic processes (i.e., $\Delta t \ll \Delta t_i$). However, this is not advisable since it is the smallest Δt_i, which sets the limit of practicality of our stochastic Monte Carlo method. An unreasonably small Δt would

use up an inordinate amount of CPU time, being very inefficient and impractical. The most efficient course is to select the computer time increment to be the same as that of the smallest basic time interval of the relevant kinetic processes.

Obviously, the smallest time interval is the reciprocal of the rate corresponding to the most active process. As a result, our CPU time depends drastically on the growth temperature in the Arrhenius form. For example, the CPU time for the standard MBE growth simulation with $R_0(\mathrm{Ga})/R_0(\mathrm{As}) = 10^3$ is roughly 15.5 min for the case of $T = 500$ K, and 120 h for the case of $T = 700$ K, on the VAX-11/785. [See Figs. 4(a) and 5(a).]

B. Different growth methods under study

We study the following MBE growth methods: (a) standard MBE, (b) growth interruption, (c) laser evaporation of the source, and (d) laser evaporation with growth interruption. In each case we study the effect on the growth of various parameters employed in the simulation (e.g., temperature and kinetic rates).

In the standard MBE growth simulation the substrate is impinged upon by gallium atoms and arsenic molecules. For a gallium atom to successfully adsorb on the surface it must be supported by at least one As atom in the layer directly beneath it. The program randomly picks two integers which provide the x and y coordinates of a possible adsorption site for an atom. The deposition of the As_2 molecule onto the surface is as follows. At first, a random site is chosen to see if it is possible to adsorb a single As atom there. If there is at least one gallium atom in the lower layer that supports that As atom, the simulation program then proceeds to find all the next-nearest-neighbor coordinates within the same layer and the next nearest underlying layer. The next-nearest-neighbor sites are the possible sites which the second partner of the arsenic molecule can occupy. Each of these sites is tested to see if it is vacant and supported from the layer below by at least one gallium atom. If there is a multiple number of possible sites for the second arsenic atom to reside on, the choice is made randomly with equal probability for all the available sites. If there are no sites which are supported, arsenic adsorption does not take place, and a search is made for a possible adsorption site in the next possible layer above.

In simulating growth interruption we proceed as in the standard MBE method, except that the deposition of the Ga and As sources is halted for some interval of time during which only the migration of atoms in the growth front takes place. Thus, growth interruption is equivalent to annealing, except that an annealing procedure is usually carried out for a prolonged period of time (on the order of hours or days) and at a different temperature from the growth temperature.

The laser evaporation technique is rather novel.[13] In this technique, the source material of the anion species (e.g., bulk arsenic) is energetically excited by a laser. This enables us to obtain anion atoms instead of molecules which are thermally obtained and are normally used as the source beam in MBE. This technique to obtain arsen-
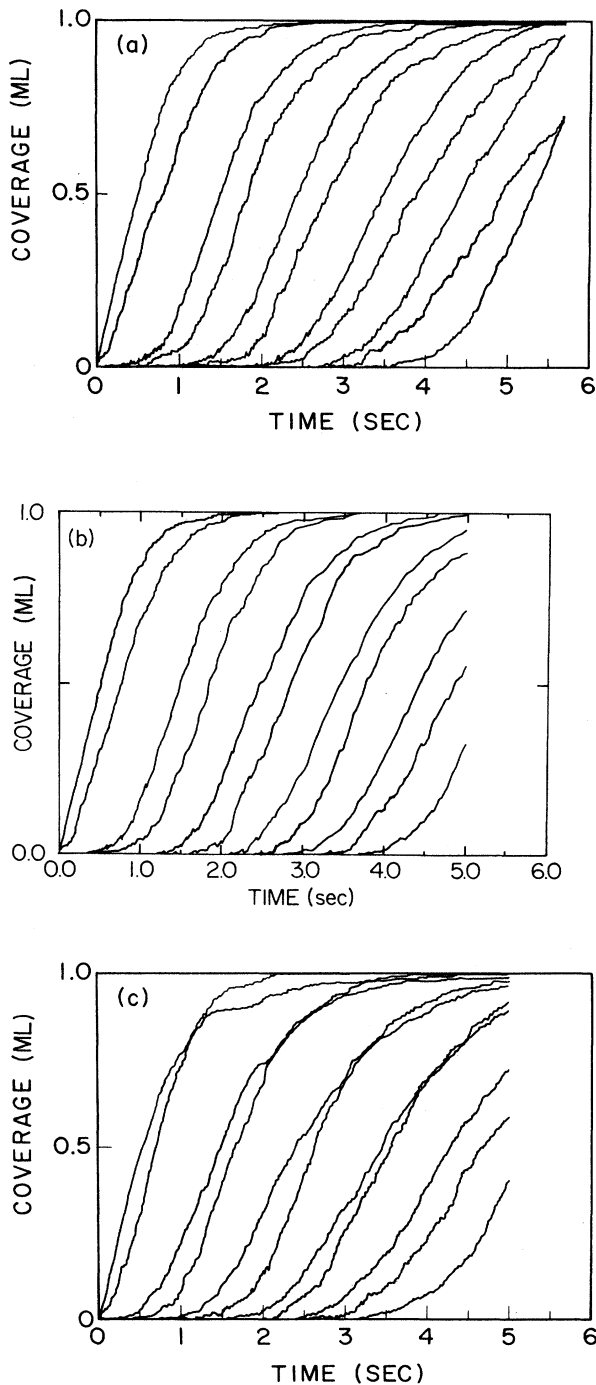
FIG. 5. The multilayer growth profile for the standard MBE growth method. The temperature is $T = 700$ K and the prefactor ratios $R_0(\mathrm{Ga})/R_0(\mathrm{As})$ are (a) 10^3, (b) 1, (c) 10^{-3}. The initial growth profile is that of the first layer of gallium growth.

ic atoms prior to impingement is expected to make the MBE growth easier. In order to incorporate this feature into our growth simulation, we alter our program, relaxing the rather stringent conditions on the adsorption of the arsenic species. Namely, we impinge As atoms (instead of molecules) onto the surface, and render the adsorption similar to that of Ga atoms.

In addition we study the qualitative trends in the growth profile when both growth interruption and laser evaporation are used in MBE.

Finally, we investigate the effects arising from the change in magnitude of the diffusive prefactor in the Arrhenius form for the rates, namely $R_0(\text{As})$ and $R_0(\text{Ga})$. We study the cases when their relative ratios are 10^3, 1, and 10^{-3}. The prefactor ratios are a measure of the temperature-independent relative hopping "activity" of the corresponding species. This analysis can illuminate whether it is the high diffusive "activity" of either the cation or the anion which leads to good epitaxial growth.

III. DISCUSSION OF RESULTS

A total of 24 growth profiles were produced with our simulation program. One set of data was obtained with a temperature of $T = 500$ K and another set at a higher temperature of $T = 700$ K. At each temperature simulation runs were made for three different cation-anion diffusion prefactor ratios of 10^3, 1, and 10^{-3}. The total computing time involved is fairly large—a rough estimate would be about 3000 h on a VAX-11/785 machine. All these runs were performed for the following growth methods: (i) standard MBE, (ii) growth interruption, (iii) laser evaporation, and (iv) growth interruption and laser evaporation.

With this data set it is possible to observe the qualitative trends as the temperature is increased and as the $R_0(\text{Ga})/R_0(\text{As})$ ratio of the temperature-independent diffusive activity is altered. In the following we discuss each of these cases separately.

A. Standard MBE

For the standard MBE growth method we can observe the following basic trends at both temperatures. As the prefactor ratio $R_0(\text{Ga})/R_0(\text{As})$ decreases so does the quality of the growth profile. This suggests that a relatively high cation diffusion rate is crucial to promote good epitaxial growth. As one can see in Figs. 4 and 5, there is a progressive deterioration of the layer-by-layer growth sequence as the prefactor ratio is decreased. The relative inactivity of the cations leads to a crossover of the surface coverages, indicating the existence of many vacancies in the lower layers and the formation of overhangs. There are two reasons for the formation of vacancies and overhangs for the lower prefactor ratio [i.e., $R_0(\text{Ga}) < R_0(\text{As})$]. Firstly, the cation atoms are not as active, and so they do not participate as frequently in the various dynamic processes. Secondly, since the interlayer diffusion of the cations is decreased, they become likelier "targets" for the arsenic molecules to "capture" them from above; cations "caught" in this fashion are

(a) Standard MBE T = 700 K

o Layer 3 (Cation)
□ Layer 4 (Anion)
● Layer 5 (Cation)
■ Layer 6 (Anion)
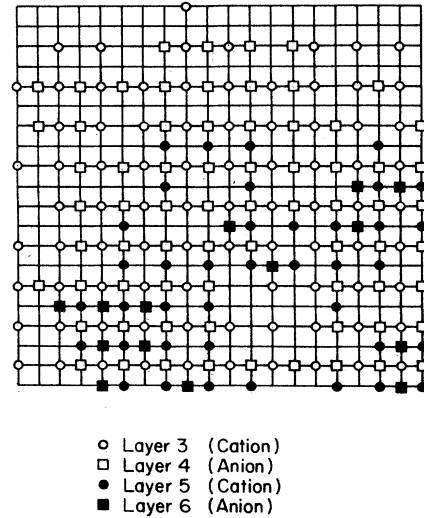
(b) Standard MBE T = 700 K
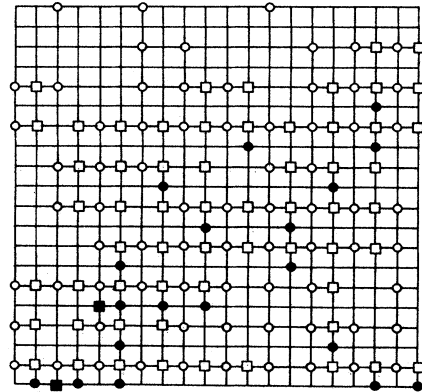
(c) Laser Evaporation T = 500 K
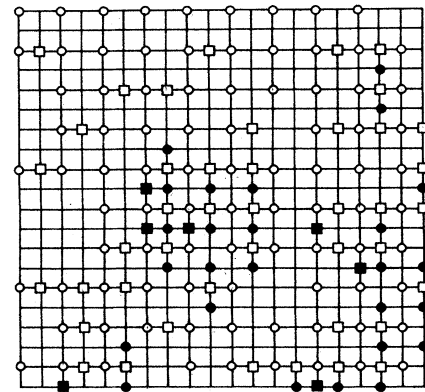
FIG. 6. The growth configuration for layers 3–6 for time $t \simeq 2.0$ s (a) standard MBE, $T = 700$ K, $R_0(\text{Ga})/R_0(\text{As}) = 10^3$; (b) standard MBE, $T = 700$ K, $R_0(\text{Ga})/R_0(\text{As}) = 10^{-3}$; (c) laser evaporation $T = 500$ K, $R_0(\text{Ga})/R_0(\text{As}) = 10^3$.

most likely supporting two arsenic atoms in the upper layer. Once a cation is supporting an atom in the upper layer, they can no longer participate in any diffusive process (i.e., they become "frozen" at particular sites for some time). This explains the existence of the vacancies at lower layers and the corresponding existence of overhangs, where the coverage of a higher layer is greater than that of a lower one.

When we compare the $R_0(Ga)/R_0(As) = 1000$ results for $T = 500$ and 700 K we see that, as expected, the higher temperature leads to an improved growth profile. Since overall the diffusive rates are greater at the higher temperature, the atoms are allowed to settle down quickly at cluster edges, thus providing a good base for epitaxial growth.

A snapshot of the growth configuration for layers 3–6 is given for a temperature of $T = 700$ K for a prefactor ratio of $R_0(Ga)/R_0(As) = 10^3$ and 10^{-3} in Figs. 6(a) and 6(b). For purposes of comparison we present the growth profile and a snapshot of the growth configuration for the case of no diffusion in Figs. 7(a) and 7(b). A comparison of these results indicates that in the no-diffusion case

(a)

(b) No Diffusion

o Layer 3 (Cation)
□ Layer 4 (Anion)
● Layer 5 (Cation)
■ Layer 6 (Anion)
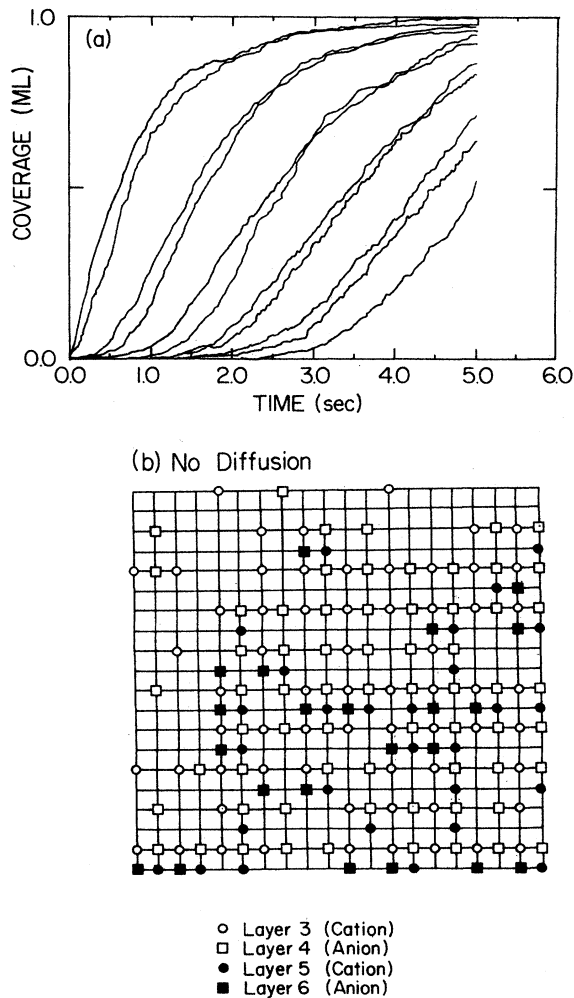
FIG. 7. The no-diffusion case. (a) The growth profile. (b) The resulting growth configuration for layers 3–6 for time $t \simeq 2.0$ s.
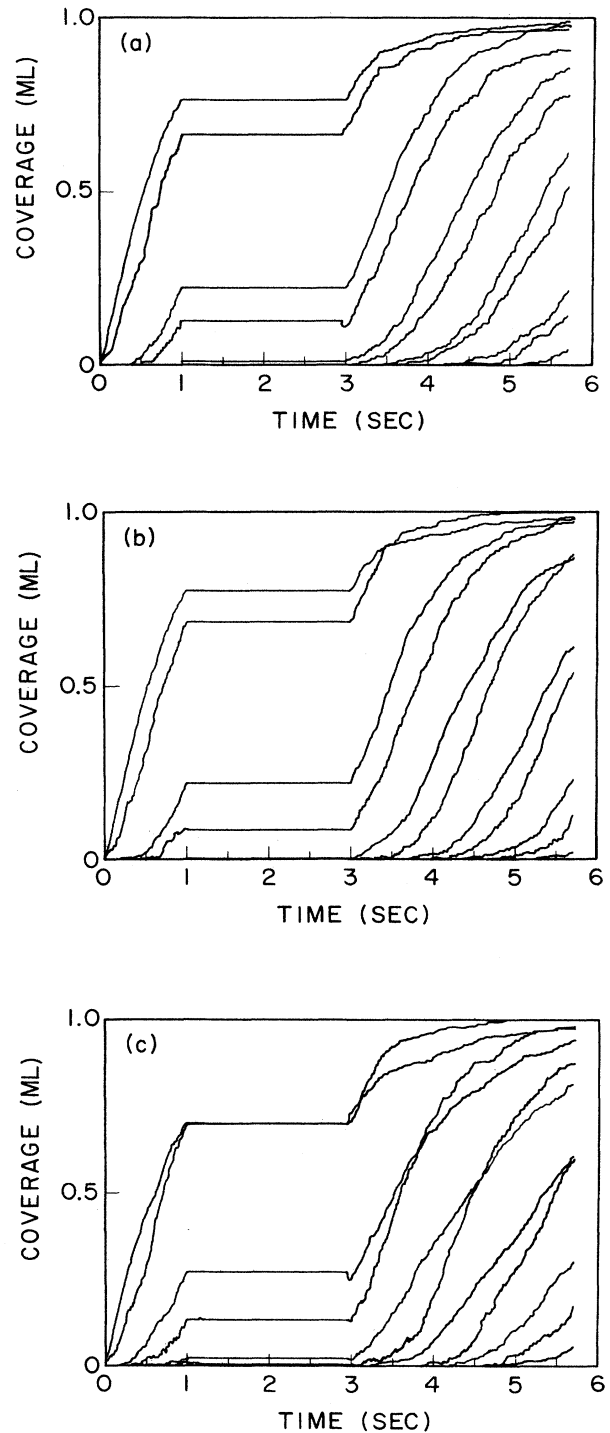
FIG. 8. The multilayer growth profile for the growth interruption method. The temperature is $T = 500$ K and the prefactor ratios $R_0(Ga)/R_0(As)$ are (a) 10^3, (b) 1, (c) 10^{-3}. The initial growth profile is that of the first layer of gallium growth.

higher layers are occupied at earlier times, and that the resulting growth configuration is rather "porous."

B. Growth interruption

The same general trends are observed in the data set for growth interruption. There are no significant changes
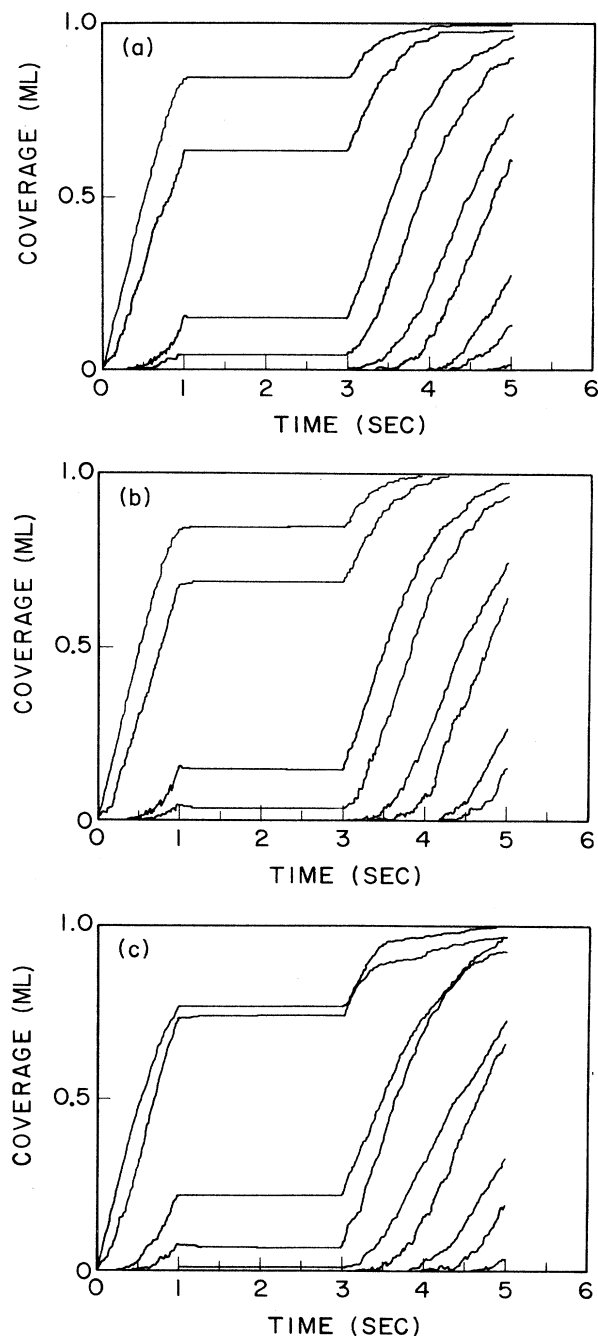
FIG. 9. The multilayer growth profile for the growth interruption method. The temperature is $T = 700$ K and the prefactor ratios $R_0(Ga)/R_0(As)$ are (a) 10^3, (b) 1, (c) 10^{-3}. The initial growth profile is that of the first layer of gallium growth.

as the deposition of the cations and anions are halted for a period of one second from $t = 2$ to 3 s. Some minor improvements are obtained during the growth interruption window, as can be seen in Figs. 8 and 9, where atoms in a higher layer make an interlayer hop downward promoting epitaxial growth. Improvements in the growth profile of this type are easily detectable as correlated decreases in surface coverage with a corresponding increase in coverage two layers below. The aim of growth interruption is to allow the atoms on the lattice to hop around and settle down to provide a good base for epitaxial growth. However, for the parameter values chosen in our simulation, it seems that there is no substantially significant improvement. The reason for the relative ineffectiveness of growth interruption in our simulation is that there is not a significant number of candidate atoms to participate in the various diffusive processes. Thus there are only a few atoms on the lattice which settle down by interlayer hops downwards to promote a better layer-by-layer growth mode.

In contrast to our results, the growth interruption method yields significant improvement in the growth profile in molecular-dynamics (MD) simulations of Lennard-Jones systems.[14] This is most likely due to the fact that in a Lennard-Jones system the atomic mobility is very high. Also, in the MD simulation the atoms are not fixed at prescribed lattice sites and are allowed a greater degree of freedom. All the pairwise interactions are taken into account so that the corresponding Newtonian dynamics ensures that the particles participate in a wide variety of diffusive processes including bulk diffusion. This facilitates the breaking up of large clusters, the subsequent diffusion of edge atoms, and various other processes, providing more candidates for interlayer hops downward promoting the epitaxial growth during interruption. In our simulation we limit the number of diffusion processes from a given site in the lattice-gas model, and employ an "edge-progression" model neglecting bulk and cluster diffusion. In simulating the growth of a compound semiconductor, these are probably not such drastic approximations since one expects less diffusive activity from atoms in semiconducting systems than from atoms making up an inert gas.

C. Laser evaporation

For the case of laser evaporation we see that, unlike the standard MBE growth method, an improved epitaxial growth is obtained for a lower prefactor ratio [i.e., $R_0(Ga) < R_0(As)$]. This is evident from the growth profiles in Figs. 10 and 11. The crossover of different layers becomes less pronounced for both temperatures $T = 500$ and 700 K. This trend results from the two competing elements of this simulation which affect the arsenic layer coverages in the growth profile.

(1) In the laser evaporation method we relax the rather stringent conditions existing for arsenic deposition in the standard MBE growth. Since the anion species are now impinging upon the surface as atoms, they can easily be incorporated at the growth front.

(2) However, for each successful deposition of an arsen-

ic atom we have only one atom, whereas in the case of the standard MBE method we had two atoms. Thus, effectively the contribution to the surface coverage is reduced by a factor of 2.

The laser evaporation data set indicates that the effect described above in (2) seems to dominate over the effect described in (1), particularly for large prefactor ratios [i.e., $R_0(\text{Ga}) > R_0(\text{As})$]. Due to the resulting low cover-
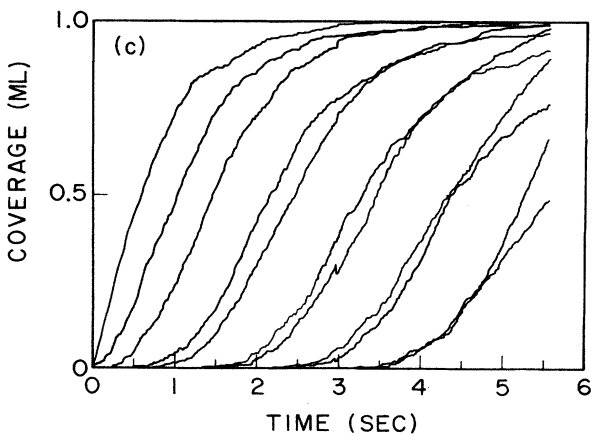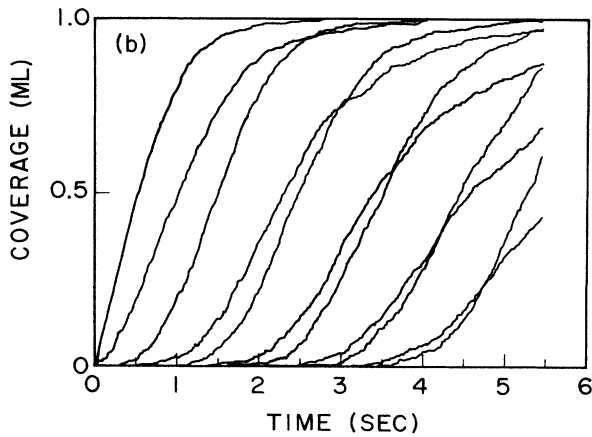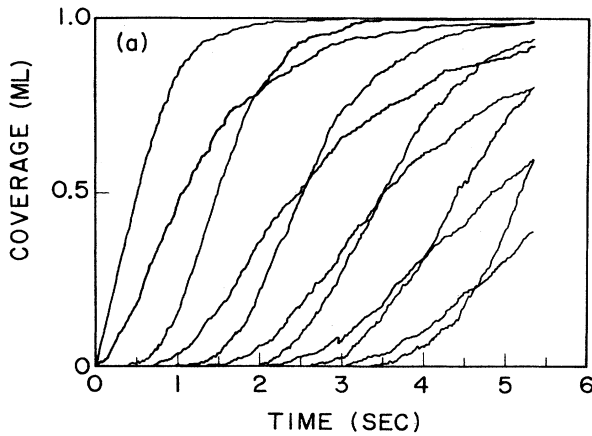
FIG. 10. The multilayer growth profile for the laser evaporation method. The temperature is $T = 500$ K and the prefactor ratios $R_0(\text{Ga})/R_0(\text{As})$ are (a) 10^3, (b) 1, (c) 10^{-3}. The initial growth profile is that of the first layer of gallium growth.
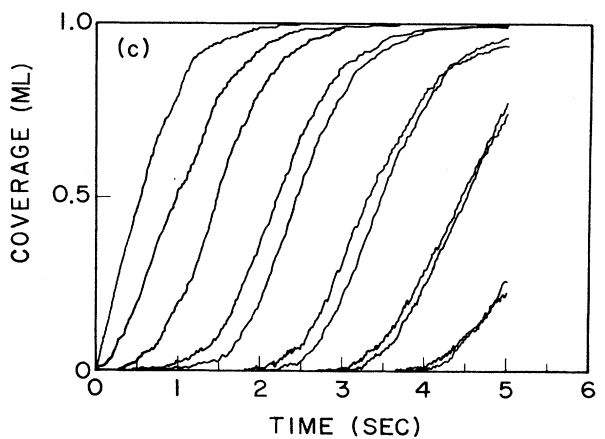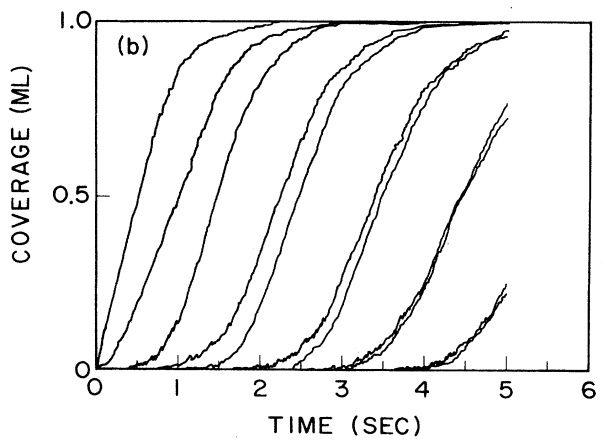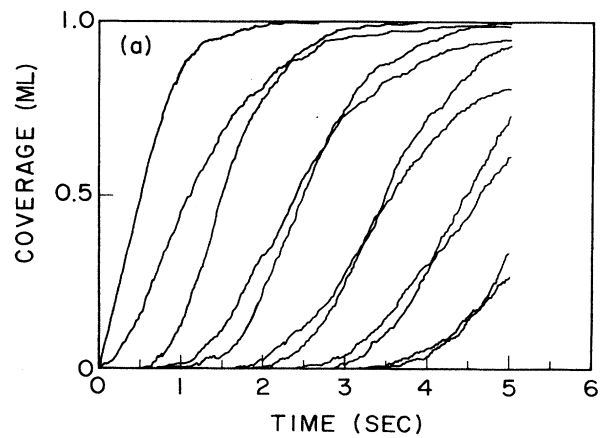
FIG. 11. The multilayer growth profile for the laser evaporation method. The temperature is $T = 700$ K and the prefactor ratios $R_0(\text{Ga})/R_0(\text{As})$ are (a) 10^3, (b) 1, (c) 10^{-3}. The initial growth profile is that of the first layer of gallium growth.

age of the arsenic layers many vacancies and overhangs are created.

For lower prefactor ratios we see that the growth profile improves greatly. This occurs due to the relative

increase of the diffusive activity of the arsenic atoms. Now the layer-by-layer growth is promoted as arsenic atoms in higher layers cascade down to lower layers. This enhances the arsenic coverages for a given time,
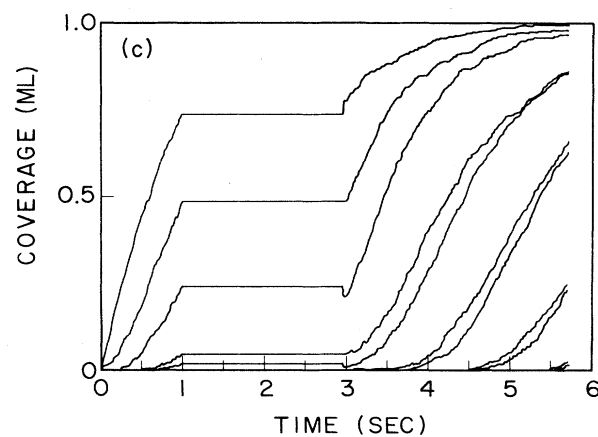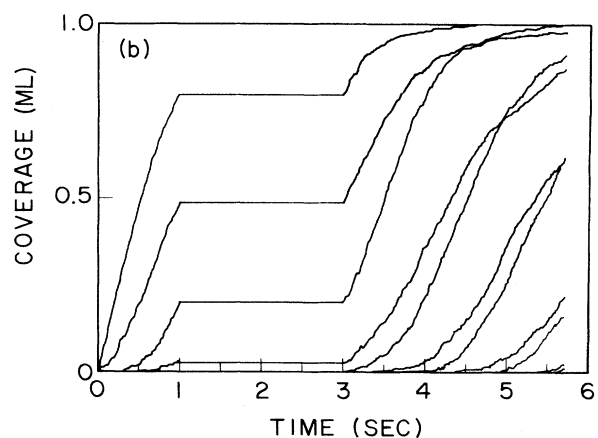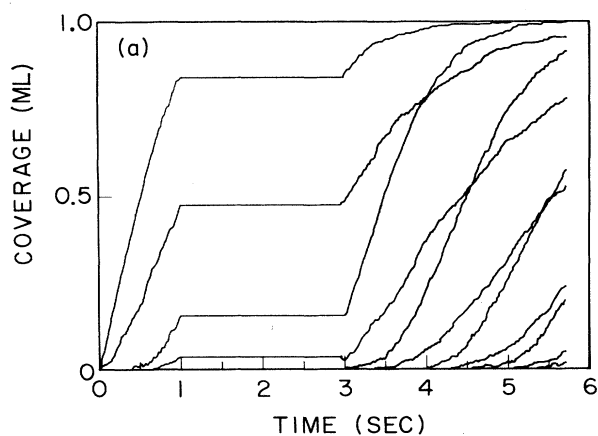
FIG. 12. The multilayer growth profile for laser evaporation and growth interruption methods combined. The temperature is $T = 500$ K and the prefactor ratios $R_0(\text{Ga})/R_0(\text{As})$ are (a) 10^3, (b) 1, (c) 10^{-3}. The initial growth profile is that of the first layer of gallium growth.
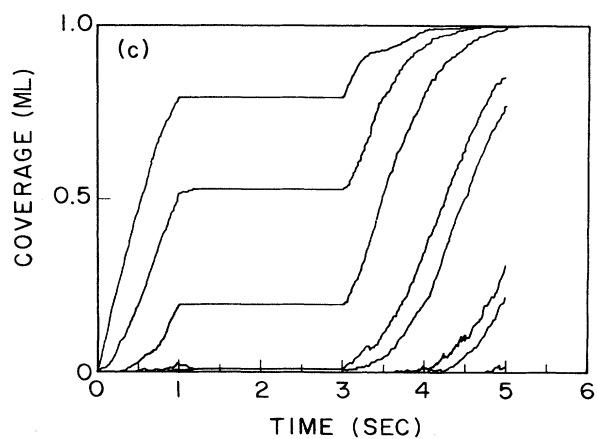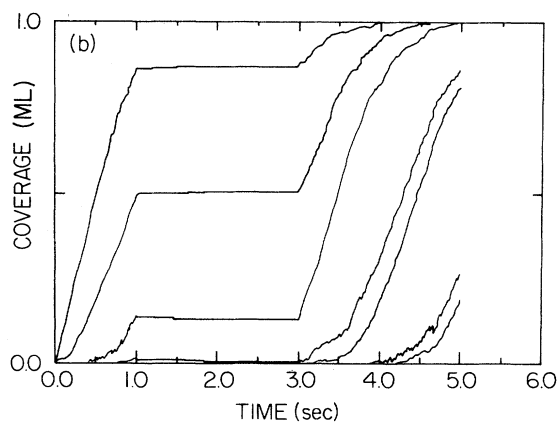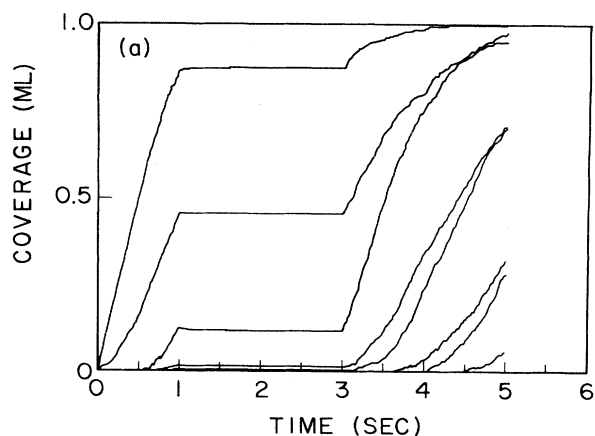
FIG. 13. The multilayer growth profile for laser evaporation and growth interruption methods combined. The temperature is $T = 700$ K and the prefactor ratios $R_0(\text{Ga})/R_0(\text{As})$ are (a) 10^3, (b) 1, (c) 10^{-3}. The initial growth profile is that of the first layer of gallium growth.

overcompensating the effect outlined in (2) above.

At first one might expect that the results in Figs. 10 and 11 should be symmetrical with respect to the prefactor ratios 10^3 and 10^{-3}, since the adsorptions of the cation and anion species are treated equivalently. However, this is not the case since we always start with an As-terminated substrate to initiate the growth front. An additional source of asymmetry is the fact that in our simulation we scale the time by fixing the Ga coverage rate at one monolayer per second, whereas the adsorption of the anions is never put under such a constraint.

D. Growth interruption and laser evaporation

As in the standard MBE method the effect of introducing the growth interruption window into the laser evaporation growth method has no significant effect on the growth profile, except for some minor improvements. The general trends observed are the same as described earlier for the laser evaporation data set (see Figs. 12 and 13).

IV. CONCLUSIONS

Using the stochastic Monte Carlo method we have shown our simulation results for epitaxial growth of a compound semiconductor. In fact, the simplicity of this technique makes it an ideal tool for obtaining a qualitative idea about how various kinetic factors affect the growth profile. We feel that this technique is particularly well suited for studying growth modifications due to variations and alterations of the standard MBE process.

If the simulation program is written in a sufficiently modular form, the introduction of many possible modifications to the standard MBE growth method is greatly facilitated. For example, one might consider the consequences of introducing a third species into the growth process. One may ascribe to this arbitrary third atom a variety of *ad hoc* attributes. The aim of such a simulation would be to find a subset of physically realistic properties which would promote epitaxial growth. For instance, we might envision the following scenario where the third species acts as an inert "capping" layer, covering a large fraction of the growth front belonging to high layer numbers. We want the newly introduced atoms to be relatively inert since we do not want them to be chemisorbed into the lattice matrix. It follows that the impinging source atoms occupy all sites belonging to low layer numbers first. After the lowest layer is completed, the capping atoms must be induced to evaporate and expose the growth front for impingement by the source atoms to build up the next layer.

In this paper the variations on the standard growth method we considered were introducing a growth interruption window, and evaporation of the anion species prior to impingement on the growth front. Recording the coverages for each layer as a function of time provides us with a record of the multilayer growth profile for later study, and allows us to determine if some particular alteration on the standard growth process leads to an improved epitaxial growth mode.

Before we conclude we should point out that simulations such as the one presented here should be considered as feasibility studies at this stage. Due to the many assumptions and approximations inherent in such simulations (some of which are uncontrolled and others whose validity cannot be tested *a priori*), and due to the small size and the limited time employed in such simulations (because of practicality), we believe that one could only make qualitative remarks about the general trends in growth as different controlling parameters are varied. For example, in the lattice MC simulation used in this paper and in other recent publications,[5-9] one would not get either the amorphous metastable growth at low temperatures or the rough and interdiffused growth at high temperatures. This is the reason why we restricted ourselves to studying the epitaxial window (500–700 K) for GaAs growth. Some of the problems in such simulations (e.g., small size and time) could probably be avoided with increasing power and efficiency of supercomputing. But, other problems such as the lack of information about various kinetic rates cannot be solved theoretically. We clearly need more experimental information on the kinetic rates before a truly quantitative model for MBE growth can be developed. Since the nature of growth depends crucially on the diffusion rates of various atomic species at the growth front, we feel that our lack of precise knowledge of such rates makes any quantitative attempt at understanding the growth of any *particular material* quite meaningless. The purpose of this rather long paper has been to establish the stochastic MC technique as a numerical tool and to provide a detailed qualitative feel for how the various kinetic processes affect the growth quality.

ACKNOWLEDGMENTS

[1]R. F. Abraham and G. M. White, J. Appl. Phys. **41**, 1841 (1970).

[2]R. C. Feber, L. D. F. Allen, and D. Grimmer, J. Vac. Sci. Technol. **8**, 397 (1970).

[3]A. C. Adams and K. A. Jackson, J. Cryst. Growth **13/14**, 144 (1972); see also, A. Kobayashi and S. Das Sarma, Phys. Rev. B **37**, 1039 (1987).

[4]J. Salik, J. Appl. Phys. **57**, 5017 (1985).

[5]S. V. Ghaisas and A. Madhukar, Phys. Rev. Lett. **56**, 1066 (1986).

[6]A. Madhukar, Surf. Sci. **132**, 344 (1983).

[7]S. V. Ghaisas and A. Madhukar, J. Vac. Sci. Technol. B **3**, 540 (1985).

[8]A. Madhukar and S. V. Ghaisas, Appl. Phys. Lett. **47**, 247

(1985).

[9]S. Clarke and D. D. Vvedensky, Phys. Rev. Lett. **58**, 2235 (1987).

[10]S. M. Paik and S. Das Sarma, Phys. Rev. B **39**, 1224 (1989); S. Das Sarma, S. M. Paik, K. E. Khor, and A. Kobayashi, J. Vac. Sci. Technol. B **5**, 1179 (1987).

[11]See, for example, W. A. Harrison, *Electronic Structure and the Properties of Solids* (Freeman, San Francisco, 1980).

[12]S. M. Paik, S. Das Sarma, Phys. Rev. B **39**, 9793 (1989).

[13]See, for example, J. T. Cheung and H. Sankur, CRC Crit. Rev. Solid State Mater. Sci. (to be published), and references therein.

[14]A. Kobayashi, S. M. Paik, and S. Das Sarma, J. Vac. Sci. Technol. B **6**, 1145 (1988).